Design of Periodic Acoustic Barriers Using an Evolutionary Topological Optimization Procedure

Rodrigo L. Pereira, Lidy Marcela Anaya Jaimes, Renato Pavanello

DESIGN OF PERIODIC NOISE BARRIERS USING THE BI-DIRECTIONAL EVOLUTIONARY STRUCTURAL OPTIMIZATION METHOD

Rodrigo L. Pereira[1] **Marcela Anaya-Jaimes**[1] **Renato Pavanello**[1]
Department of Computational Mechanics, School of Mechanical Engineering,
University of Campinas, Rua Mendeleyev, 200, 13083-860 Campinas, Brazil
pereira@fem.unicamp.br, lidy@fem.unicamp.br, pava@fem.unicamp.br

ABSTRACT

In the past few years, acoustic-mechanical devices have become widely used, which increased the demand for noise control solutions. One of the approaches to solve such problems consists in designing noise barriers. However, finding the best topology for these barriers can be a complex task. In this work it is proposed a methodology to design periodic noise barriers, composed of rigid materials, using the bi-directional evolutionary structural optimization (BESO) method. The acoustic problem is modeled using the Helmholtz equation and solved by the finite element procedure, while a material interpolation scheme is used for switching acoustic and rigid elements. The optimization problem is defined as the minimization of the average square pressure amplitude in a specific region of the acoustic domain, while the volume of the barrier is reduced. The sensitivity analysis was carried out by the gradient of the objective function with respect to the design variable. Two cases are presented in order to show the capabilities of the proposed approach. In the first one, periodic conditions are imposed in the entire system, while in the second non-periodic conditions are considered. The results showed that, although the barrier volume was reduced by 35% in both cases, the objective function decreased at least 68.80%.

1. INTRODUCTION

In the last decades, topology optimization methods have become powerful engineering tools since they provide non-intuitive structure designs for a large number of applications. Generally, what is sought is a lighter structure that is also able to enhance a few characteristics of the system, making the design even less costly. After the development and popularization of computing, many methods arose in order to make use of topology optimization.

The Evolutionary Structural Optimization (ESO) method, first introduced by Xie and Steven in the early 1990s [1], has as premise the removal of inefficient material from the structure. However, this could also result in non-optimal geometries due to inappropriate initial design settings [2]. Later, the Bi-directional Evolutionary Structural Optimization (BESO) method, proposed by Yang et al. [3], made possible not only to remove but also add elements to the structure during the optimization process. Shortly thereafter, the so-called new BESO algorithm [4] has been used in many works, since also provides solutions for some important numerical problems, such as checkerboard pattern and mesh-dependence. All these improvements made the method even more popular and highly used in many engineering applications [5, 6].

Acoustic-mechanical devices (AMDs), like microphones and speakerphones, are increasingly familiar and so is the noise control situation. As a result, the interest of many researchers, whose main focus is the design of acoustic barriers, enhanced. Due to the vast applicability of such acoustic components, going from houses, hospitals and schools to the automotive industry, for example, a great number of techniques have been implemented to design such systems.

It became common to design acoustic barriers, in repetitive domains, taking into account the complexities of fluid-structure interactions [7]. However, a more simplified approach, which consists of infinitely enlarge, in a theoretical point of view, the mass density and bulk modulus of the barrier material to generate a rigid structure, has gained many supporters [8–10]. This is due to the fact that it reduces the multiphysical fluid-structure problem to an acoustical one, ruled by the Helmholtz equation.

Acoustic topology optimization (ATO) problems have been solved, using the BESO method, in the works of Vicente et al. [11] and Picelli et al. [12], but their main focus was on the structural part of the problem and, in many situations, even neglected the effects of the acoustic domain. Kook [13] and Dilgen et al. [14] also used the bi-directional optimization method, together with a mixed u/p formulation, in order to solve classical acoustic-structure problems. Finally, Azevedo et al. [15] combined the BESO approach and the rigid material approximation with the goal of maximizing the transmission loss in the internal partitions of a reactive muffler.

With this in mind and seeking to enhance the use of the bi-directional evolutionary structural topology optimization method in the context of noise attenuation, this paper aims to optimize noise barriers when subjected to periodic and non-periodic conditions. The organization of this paper is presented as follows: In section 2 the acoustic problem is formulated using the finite element approach. In section 3 the optimization problem, as well as the material interpolation scheme and the design sensitivity analysis are discussed. Also in this section, the BESO method is described in detail. Section 4 presents numerical results,

intending to demonstrate the relevance of the presented methodology. Finally, conclusions are drawn in section 5.

2. ACOUSTIC PROBLEM FORMULATION

Considering an acoustic volume Ω_f that includes the design, Ω_d, non-design, Ω_{nd}, and objective, Ω_o, domains, as illustrated in Fig. 1. The boundaries are of Dirichlet, Γ_D, Neumann, Γ_N, and Robin, Γ_R, types where it is possible to prescribe the acoustic pressure, normal gradient pressure and acoustic admittance [16], respectively, according to the system of Eqn. (1).

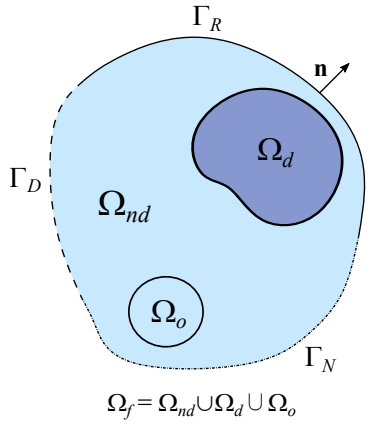

Figure 1. Acoustic continuum

$$\begin{cases} \nabla^2\tilde{p} + \dfrac{\omega^2}{c^2}\tilde{p} = 0 & \text{in} \quad \Omega_f \\ \tilde{p} = \bar{p} & \text{at} \quad \Gamma_D \\ \nabla\tilde{p}\cdot\mathbf{n} = -\rho_0\bar{a}_n & \text{at} \quad \Gamma_N \\ \nabla\tilde{p}\cdot\mathbf{n} + i\rho_0\omega\tilde{A}\tilde{p} = 0 & \text{at} \quad \Gamma_R \end{cases} \tag{1}$$

Where $\tilde{p}$ and $\bar{p}$ are, respectively, the complex and prescribed acoustic pressure, ω is the angular frequency, c is the speed of sound in air, $\mathbf{n}$ is the outward unit normal vector, ρ_0 is the fluid mass density, $\bar{a}_n$ is the prescribed normal acceleration and $\tilde{A}$ is the acoustic admittance.

In order to provide a discrete approximation of the continuum problem stated in Eqn. (1), the finite element (FE) method is considered [15–17]. Thus, multiplying the Helmholtz equation by a weight function ν and integrating on the entire fluid domain (method of weighted residual) the strong form can be written as Eqn. (2).

$$\int_{\Omega_f} \nabla^2\tilde{p}\nu \, d\Omega_f + \frac{\omega^2}{c^2}\int_{\Omega_f} \tilde{p}\nu \, d\Omega_f = 0 \tag{2}$$

Applying Green's theorem, Eqn. (2) becomes,

$$-\int_{\Omega_f} \nabla\tilde{p}\cdot\nabla\nu \, d\Omega_f + \int_{\Gamma} \nabla\tilde{p}\cdot\mathbf{n}\nu \, d\Gamma + \frac{\omega^2}{c^2}\int_{\Omega_f} \tilde{p}\nu \, d\Omega_f = 0 \tag{3}$$

for $\Gamma = \Gamma_D \cup \Gamma_N \cup \Gamma_R$. Substituting the boundary conditions presented in Eqn. (1), and knowing that $\nabla\tilde{p}\cdot\mathbf{n} = 0$ for the rigid wall case, the weak form can then be written as Eqn. (4).

$$\int_{\Omega_f} \nabla\tilde{p}\cdot\nabla\nu \, d\Omega_f + \int_{\Gamma_N} \rho_0\bar{a}_n\nu \, d\Gamma_N + \int_{\Gamma_R} i\rho_0\omega\tilde{A}\tilde{p}\nu \, d\Gamma_R - \frac{\omega^2}{c^2}\int_{\Omega} \tilde{p}\nu \, d\Omega_f = 0 \tag{4}$$

The complex acoustic pressure and its normal gradient can be rewritten in a more suitable manner,

$$\tilde{p} = \mathbf{N}\tilde{\mathbf{p}}_i, \qquad \nabla\tilde{p} = \boldsymbol{\partial}\mathbf{N}\tilde{\mathbf{p}}_i \tag{5}$$

where $\mathbf{N}$ is the FE shape function matrix, with $\boldsymbol{\partial}\mathbf{N}$ denoting its derivation, and $\tilde{\mathbf{p}}_i$ is the complex acoustic pressure vector of the ith element. With the use of Galerkin method, the weight function can be written,

$$\nu = \mathbf{N}\boldsymbol{\nu}_i, \qquad \nabla\nu = \boldsymbol{\partial}\mathbf{N}\boldsymbol{\nu}_i \tag{6}$$

where $\boldsymbol{\nu}$ is the weight function vector of the ith element. Finally, substituting Eqns. (5) and (6) in Eqn. (4) and performing the FE assembly procedure, the global dynamic system arises,

$$\mathbf{S}\tilde{\mathbf{p}} = (\mathbf{K} + i\omega\mathbf{C} - \omega^2\mathbf{M})\tilde{\mathbf{p}} = \mathbf{f} \tag{7}$$

where $\mathbf{S}$ corresponds to the system matrix and has contributions from $\mathbf{K}$, $\mathbf{C}$ and $\mathbf{M}$, denoting the acoustic stiffness, damping and mass matrices, respectively, while $\mathbf{f}$ is the acoustic load vector. Besides,

$$\mathbf{K}_i = \frac{1}{\rho_0}\int_{\Omega_f} (\boldsymbol{\partial}\boldsymbol{N})^t\boldsymbol{\partial}\boldsymbol{N} \, d\Omega_f \tag{8}$$

$$\mathbf{C}_i = \tilde{A}\int_{\Gamma_R} \mathbf{N}^t\mathbf{N} \, d\Gamma_R \tag{9}$$

$$\mathbf{M}_i = \frac{1}{\kappa}\int_{\Omega_f} \mathbf{N}^t\mathbf{N} \, d\Omega_f \tag{10}$$

$$\mathbf{f}_i = -\bar{a}_n\int_{\Gamma_N} \mathbf{N}^t \, d\Gamma_N \tag{11}$$

where the subscript i represents elementary variables. The bulk modulus of the acoustic medium is denoted by κ, which is equal to $\rho_0 c^2$.

3. RIGID BARRIER TOPOLOGY OPTIMIZATION

In this section, the optimization problem is presented, as well as the adopted material interpolation scheme, the design sensitivity analysis and the evolutionary procedure. Eqn. (12) states the topology optimization problem as the minimization of the average square acoustic pressure amplitude at Ω_o [7–9, 13] subject to restrictions stated in Eqns. (13), (14) and (15).

$$\text{Minimize:} \quad \Phi = \frac{1}{\int_{\Omega_o} d\boldsymbol{r}}\int_{\Omega_o} |\tilde{p}(\boldsymbol{r}, \chi(\boldsymbol{r}))|^2 \, d\boldsymbol{r} \tag{12}$$

$$\text{Subjected to:} \quad V^* - \frac{1}{\int_{\Omega_d} d\boldsymbol{r}}\int_{\Omega_d} \chi(\boldsymbol{r}) \, d\boldsymbol{r} = 0 \tag{13}$$

$$\mathbf{S}(\boldsymbol{\chi}(\boldsymbol{r}))\tilde{\mathbf{p}}(\boldsymbol{r}, \boldsymbol{\chi}(\boldsymbol{r})) = \mathbf{f} \tag{14}$$

$$\chi(\boldsymbol{r}) = 0 \text{ or } 1 \qquad \forall \boldsymbol{r} \in \Omega_d \tag{15}$$

Where Φ is the objective function and V^* is the imposed volume fraction, which varies from 0 to 1. Eqn. (14) exposes that $\tilde{\mathbf{p}}$ depends on the binary design variable, $\boldsymbol{\chi}$, and the position, $\boldsymbol{r}$, vectors. The elemental values of χ can only be 0 for air or 1 for rigid materials.

3.1 Material interpolation scheme

As discussed in section 2, three different regions are included in the fluid domain Ω_f (see Fig. 1). In the non-design, Ω_{nd}, and objective, Ω_o, domains the medium is air. However, in the design domain, Ω_d, the medium is composed of an acoustic barrier of rigid constitution. Following many researchers [7–10, 18], this so-called rigid material is the result of a mathematical resource in which the air density and bulk modulus are infinitely amplified, from a purely theoretical point of view, in order to generate a material where the wave is totally reflected. However, to avoid numerical singularities in the calculation of the acoustic finite element matrices, adequate values need to be chosen for these variables. In this sense, the physical properties considered are $\rho_{air} = 1.21$ kg/m^3, $\kappa_{air} = 1,42e5$ Pa, $\rho_{rigid} = 1,21e5$ kg/m^3 and $\kappa_{rigid} = 1,21e12$ Pa, where the subscripts air and $rigid$ denote air and rigid material, respectively [9]. To find the optimal distribution of rigid in Ω_d, the material interpolation scheme, presented in Eqns. (16) and (17), is adopted.

$$\frac{1}{\rho} = \frac{1}{\rho_{air}} + \chi\left(\frac{1}{\rho_{rigid}} - \frac{1}{\rho_{air}}\right) \tag{16}$$

$$\frac{1}{\kappa} = \frac{1}{\kappa_{air}} + \chi\left(\frac{1}{\kappa_{rigid}} - \frac{1}{\kappa_{air}}\right) \tag{17}$$

3.2 Design Sensitivity Analysis

It is discussed, in this section, the sensitivity numbers based on the average square acoustic pressure amplitude [7]. Thus, since $\tilde{\mathbf{p}}$ is a complex vector, it can be written as follows,

$$\tilde{\mathbf{p}} = \mathbf{p}_R + i\mathbf{p}_I \tag{18}$$

with $\mathbf{p}_R$ and $\mathbf{p}_I$ denoting real and imaginary parts of $\tilde{\mathbf{p}}$. Knowing that Φ is a function of,

$$\Phi = \Phi(\mathbf{p}_R, \mathbf{p}_I, \boldsymbol{\chi}), \tag{19}$$

the adjoint method [19] is used by the introduction of Lagrangian multipliers, $\tilde{\boldsymbol{\lambda}}$ and $\bar{\tilde{\boldsymbol{\lambda}}}$,

$$\Phi = \Phi(\mathbf{p}_R, \mathbf{p}_I, \boldsymbol{\chi}) + \tilde{\boldsymbol{\lambda}}^t(\mathbf{S}\tilde{\mathbf{p}} - \mathbf{f}) + \bar{\tilde{\boldsymbol{\lambda}}}^t(\bar{\mathbf{S}}\bar{\tilde{\mathbf{p}}} - \bar{\mathbf{f}}) \tag{20}$$

where the over bars denote complex conjugates. It is important to note that all pressure vectors are also dependent on $\boldsymbol{\chi}$, but this was not shown in Eqns. (18), (19) and (20) in order to simplify the notation.

Taking the derivative of Eqn. (20), with respect to the design domain variable, yields,

$$\begin{aligned}\frac{d\Phi}{d\chi} = \frac{\partial\Phi}{\partial\chi} + \frac{\partial\Phi}{\partial\mathbf{p}_R}\frac{\partial\mathbf{p}_R}{\partial\chi} + \frac{\partial\Phi}{\partial\mathbf{p}_I}\frac{\partial\mathbf{p}_I}{\partial\chi} + \\ \tilde{\boldsymbol{\lambda}}^t\left(\frac{\partial\mathbf{S}}{\partial\chi}\tilde{\mathbf{p}} + \mathbf{S}\frac{\partial\mathbf{p}_R}{\partial\chi} + i\mathbf{S}\frac{\partial\mathbf{p}_I}{\partial\chi} - \frac{\partial\mathbf{f}}{\partial\chi}\right) + \\ \bar{\tilde{\boldsymbol{\lambda}}}^t\left(\frac{\partial\bar{\mathbf{S}}}{\partial\chi}\bar{\tilde{\mathbf{p}}} + \bar{\mathbf{S}}\frac{\partial\mathbf{p}_R}{\partial\chi} - i\bar{\mathbf{S}}\frac{\partial\mathbf{p}_I}{\partial\chi} - \frac{\partial\bar{\mathbf{f}}}{\partial\chi}\right)\end{aligned} \tag{21}$$

which becomes,

$$\begin{aligned}\frac{d\Phi}{d\chi} = \frac{\partial\Phi}{\partial\chi} + \tilde{\boldsymbol{\lambda}}^t\left(\frac{\partial\mathbf{S}}{\partial\chi}\tilde{\mathbf{p}} - \frac{\partial\mathbf{f}}{\partial\chi}\right) + \bar{\tilde{\boldsymbol{\lambda}}}^t\left(\frac{\partial\bar{\mathbf{S}}}{\partial\chi}\bar{\tilde{\mathbf{p}}} - \frac{\partial\bar{\mathbf{f}}}{\partial\chi}\right) + \\ \left(\frac{\partial\Phi}{\partial\mathbf{p}_R} + \tilde{\boldsymbol{\lambda}}^t\mathbf{S} + \bar{\tilde{\boldsymbol{\lambda}}}^t\bar{\mathbf{S}}\right)\frac{\partial\mathbf{p}_R}{\partial\chi} + \\ \left(\frac{\partial\Phi}{\partial\mathbf{p}_I} + i\tilde{\boldsymbol{\lambda}}^t\mathbf{S} - i\bar{\tilde{\boldsymbol{\lambda}}}^t\bar{\mathbf{S}}\right)\frac{\partial\mathbf{p}_I}{\partial\chi}.\end{aligned} \tag{22}$$

Since the Lagrangian multipliers can assume any number, the unknown expressions involving $\frac{\partial\mathbf{p}_R}{\partial\chi}$ and $\frac{\partial\mathbf{p}_I}{\partial\chi}$ can be eliminated by satisfying Eqns. (23) and (24).

$$\tilde{\boldsymbol{\lambda}}^t\mathbf{S} + \bar{\tilde{\boldsymbol{\lambda}}}^t\bar{\mathbf{S}} = -\frac{\partial\Phi}{\partial\mathbf{p}_R} \tag{23}$$

$$i\tilde{\boldsymbol{\lambda}}^t\mathbf{S} - i\bar{\tilde{\boldsymbol{\lambda}}}^t\bar{\mathbf{S}} = -\frac{\partial\Phi}{\partial\mathbf{p}_I} \tag{24}$$

Multiplying Eqn. (24) by $-i$, adding the result to Eqn. (23) and transposing both sides (knowing that $\mathbf{S}^t = \mathbf{S}$), the adjoint equation is found,

$$\mathbf{S}\tilde{\boldsymbol{\lambda}} = -\frac{1}{2}\left(\frac{\partial\Phi}{\partial\mathbf{p}_R} - i\frac{\partial\Phi}{\partial\mathbf{p}_I}\right)^t \tag{25}$$

with $\tilde{\boldsymbol{\lambda}}$ being the solution of the adjoint equation and with the right side of Eqn. (25) defined as the adjoint load. Finally, it is possible to rewrite Eqn. (22) in its final form,

$$\alpha_i = -\frac{d\Phi}{d\chi} = -\left\{\frac{\partial\Phi}{\partial\chi} + 2Re\left[\tilde{\boldsymbol{\lambda}}^t\left(\frac{\partial\mathbf{S}}{\partial\chi}\tilde{\mathbf{p}} - \frac{\partial\mathbf{f}}{\partial\chi}\right)\right]\right\} \tag{26}$$

where α_i denotes the sensitivity number of the ith element. Also, it is noticeable that (26) has received a minus sign on its right side, which acts as a corrector of the BESO method towards minimization of the objective function.

Making use of the material interpolation scheme, Eqns. (16) and (17), the derivatives stated at Eqn. (26) can be easily written, at the elementary level, as follows,

$$\frac{\partial\Phi}{\partial\chi} = 0, \qquad \frac{\partial\mathbf{f}}{\partial\chi} = 0 \tag{27}$$

$$\frac{\partial\mathbf{S}}{\partial\chi} = \frac{\partial\mathbf{K}}{\partial\chi} + i\omega\frac{\partial\mathbf{C}}{\partial\chi} - \omega^2\frac{\partial\mathbf{M}}{\partial\chi} \tag{28}$$

with,

$$\frac{\partial\mathbf{C}}{\partial\chi} = 0 \tag{29}$$

$$\frac{\partial\mathbf{K}}{\partial\chi} = \left(\frac{1}{\rho_{rigid}} - \frac{1}{\rho_{air}}\right)\int_{\Omega_d}(\boldsymbol{\partial N})^t\boldsymbol{\partial N}\, d\Omega_d \tag{30}$$

$$\frac{\partial\mathbf{M}}{\partial\chi} = \left(\frac{1}{\kappa_{rigid}} - \frac{1}{\kappa_{air}}\right)\int_{\Omega_d}\mathbf{N}^t\mathbf{N}\, d\Omega_d. \tag{31}$$

Knowing that,

$$|\tilde{p}|^2 = p_R^2 + p_I^2 \tag{32}$$

$$p_R = \mathbf{N}\mathbf{p}_R \tag{33}$$

$$p_I = \mathbf{N}\mathbf{p}_I \tag{34}$$

the adjoint load can also be rewritten in an integral form as Eqn. (35).

$$-\frac{1}{2}\left(\frac{\partial\Phi}{\partial\mathbf{p}_R} - i\frac{\partial\Phi}{\partial\mathbf{p}_I}\right)^t = -\left(\frac{1}{\int_{\Omega_o} d\Omega_o}(\mathbf{p}_R^t - i\mathbf{p}_I^t)\int_{\Omega_o}\mathbf{N}^t\mathbf{N}\, d\Omega_o\right)^t \tag{35}$$

Since the optimization of periodic noise barriers is examined, an additional procedure needs to be performed in order to ensure the same topology in all barrier cells. In that way, when more than one cell is considered, a periodic vector of sensitivities is calculated by the following procedure:

1. Calculate all the sensitivity numbers inside the design domain using Eqns. (25) to (35).

2. Separate the sensitivity numbers by cell vectors, in order to identify the first, second, down to the last elements, of each periodic cell.

3. Average the sensitivity numbers of all the firsts, seconds, down to the last elements, and store those values inside another variable, called periodic sensitivity vector.

4. Use this new vector throughout the BESO methodology.

All this process ensures that the same barrier is obtained independently of the amount of cells considered.

3.3 Bi-directional Evolutionary Procedure

This section presents the Bi-directional evolutionary structural optimization (BESO) method related with acoustic problems [4, 5, 13, 15]. The main steps of the methodology are given as follows:

1. Execute the finite element procedure using Eqns. (7) to (11). This analysis should be performed in order to find the acoustic pressure in the fluid domain. At this point, it is important to differentiate air and rigid elements, that encompass the design domain, by attributing the correct physical properties to each case (see section 3.1).

2. Carry out the sensitivity analysis. In this case the sensitivity numbers were validated by comparing them to the ones obtained by the finite differences method.

3. Apply the filter scheme, Eqns. (36) to (38), in order to deal with numerical problems that arises with the use of low order elements [4, 20].

$$\alpha_j = \sum_{i=1}^{M} w_i\alpha_i \tag{36}$$

$$w_i = \frac{1}{M-1}\left(1 - \frac{r_{ij}}{\sum_{i=1}^{M} r_{ij}}\right) \tag{37}$$

Where α_j denotes the sensitivity number of the jth node, M is the total number of elements connected to the jth node, w_i is the weight factor of the ith element, with $\sum_{i=1}^{M} w_i = 1$, and r_{ij} corresponds to the distance between the center of the ith element and the jth node. Additionally, a length scale, r_{min}, is defined with the goal of identify the nodes that contribute to the sensitivity of the ith element as follows,

$$\alpha_i = \frac{\sum_{j=1}^{tnd} w(r_{ij})\alpha_j}{\sum_{j=1}^{tnd} w(r_{ij})} \tag{38}$$

with tnd being the total number of nodes that has influence over α_i and $w(r_{ij})$ is the linear weight factor determined by $r_{min} - r_{ij}$, for all nodes inside the subdomain imposed by r_{min}.

4. Apply the sensitivity history. One of the main characteristics of the BESO method consists in the usage of discrete design variables, which may cause difficulties in the convergence of the objective function and its corresponding topology. One way to solve this issue is to average the sensitivity numbers with its historical information. A way to do that is by the application of Eqn. (39),

$$\alpha_i = \frac{\alpha_i^{it} + \alpha_i^{it-1}}{2} \tag{39}$$

where superscript it refers to the current iteration.

5. Define the volume target for the next iteration,

$$V_{it+1} = V_{it}(1 \pm ER) \tag{40}$$

where V_{it} is the volume fraction of the iteration it and ER is the evolutionary rate. When the final volume fraction, V^*, is reached, the next iterations must necessarily keep the volume constant until the stop criteria (step 7) is fulfilled.

6. Define element type. The definition of volume for the next iteration establishes a threshold for the amount of elements that will be air ($\chi = 0$) or rigid ($\chi = 1$). Looking at the sensitivity numbers in the context of minimization of the objective function, it is possible to write Eqns. (41) and (42).

$$\alpha_i \leq \alpha_{th} \quad \text{air elements} \tag{41}$$

$$\alpha_i > \alpha_{th} \quad \text{rigid elements} \tag{42}$$

Besides, another important parameter that needs to be addressed is the addition ratio, AR, which defines the additional volume that can return to the FE mesh. However, in order to restrict this amount, the maximum addition ratio, AR_{max}, is also stated. If the case $AR > AR_{max}$ happens, only some elements with the lowest α_i will be turned to air in order to respect the $AR = AR_{max}$ restriction. This fact also implies that some elements with the highest α_i will be turned to rigid, fulfilling V_{it+1} [12].

7. Repeat 1 to 6 until the final volume is reached and the stop criteria, Eqn. (43), is satisfied.

$$\frac{|\sum_{m=1}^{5}\Phi_{it-m+1} - \sum_{m=1}^{5}\Phi_{it-m-4}|}{\sum_{m=1}^{5}\Phi_{it-m+1}} \leq \tau \quad (43)$$

The variable τ denotes the allowable error tolerance.

4. NUMERICAL RESULTS

This section presents the optimization of an acoustic barrier with periodic, case 1, and non-periodic, case 2, settings. Fig. 2 illustrates the geometry considered in the examples. The gray region denotes the design domain, initially full of rigid elements. The green and white areas are the objective and non-design domain regions, respectively, composed of air elements. The entire cell has 730 mm of length and 45 mm of height, with an initial barrier of 30x27 mm^2. At boundary Γ_{in} different inputs are given in order to explore further the behavior of the optimization method when dealing with this kind of ATO problem, while Γ_{out} is considered closed in all examples.

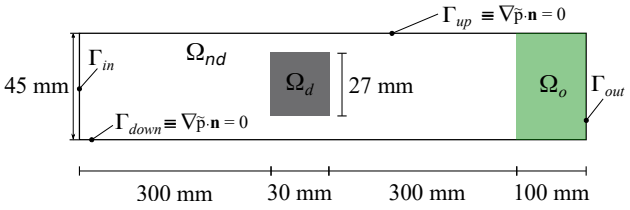

Figure 2. Geometric details of the structure adopted in the examples

4.1 Case 1: Barrier optimization in a periodic system

Fig. 3(a) shows the sound pressure field of the acoustic tube with dimensions given in Fig. 2, when subjected to a plane wave caused by an acceleration of 1 m/s^2, at Γ_{in}, and frequency of 2900 Hz. The fluid domain is discretized by 292x30 first order quadrilateral elements, which is above the minimum recommend per wavelength [16]. The speed of sound in air is 343 m/s, with the physical characteristics of air and rigid materials as stated in section 3.1. Fig. 3(b) illustrates the sound pressure field of the acoustic system with the optimized rigid barrier. The BESO parameters are: $V^* = 0.65$, $ER = 1.0\%$, $AR_{max} = 1.4\%$, $r_{min} = 10$ mm and $\tau = 0.1\%$. Fig. 3(c) is the representation of the same problem, but with three periodic cells, which makes a finite element mesh of size 292x90.

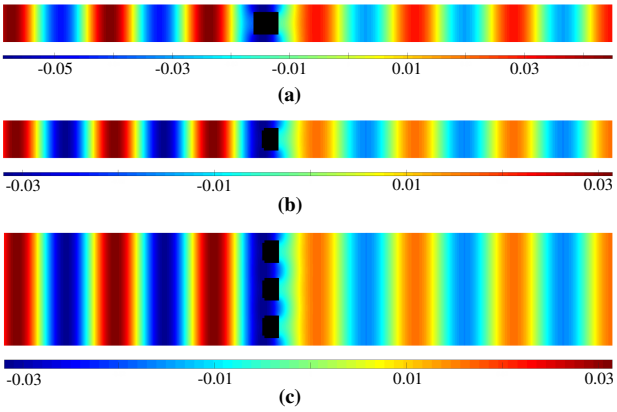

Figure 3. Sound pressure field of an acoustic tube **(a)** one cell with a non-optimized barrier **(b)** one cell with an optimized barrier **(c)** three cells and optimized barriers

It is observed from Fig. 3(b) and (c) that the same results are found after the optimization is complete due to the periodic conditions of the problem. Since the fluid domain is horizontally symmetric, it is possible to model rigid barriers with one or even half of a periodic cell, representing a significant reduction of computational cost. This becomes even clearer with the observation of Fig. 4, that presents the identical evolution of the objective function for the examples with one and three periodic cells, respectively. The barrier topology in iterations 10, 30 and 50 are also shown. The BESO method reveals great potential in the optimization of noise barriers with periodic conditions, since the average square pressure is reduced by 68.80%, while 35% of the barrier volume is also reduced. Additionally, there was no break of horizontal symmetry during the entire optimization process, resulting in a smooth behavior of the objective function.

4.2 Case 2: Optimization of a non-periodic system

Fig. 5(a) illustrates the sound pressure field of a similar acoustic tube to the one presented in section 4.1 since the geometry, acceleration and frequency are maintained. However, a wave is generated by a cylindrical source of 45 mm in length, located at the center of Γ_{in}. In this case, since the boundary is non-periodic, the entire tube needs to be analyzed or Floquet-Bloch boundary conditions would have to be imposed in order to consider the different phases between cells [21]. Since this is an early study on the behavior of the BESO method in the optimization of noise barriers, the authors choose to only consider the case presented in Fig. 5(a). It is our hope to go deeper into this topic and even study the optimization of acoustic barriers composed of poroelastic materials [22, 23] in future work. Fig. 5(b) presents the results found after the optimization takes place. The BESO parameters considered in this case are: $V^* = 0.65$, $ER = 0.6\%$, $AR_{max} = 0.8\%$, $r_{min} = 18$ mm and $\tau = 0.1\%$. It must be pointed out that despite of the non-periodic setting, the barrier was considered as three cells, to which were applied the procedures described at the end of section 3.2.

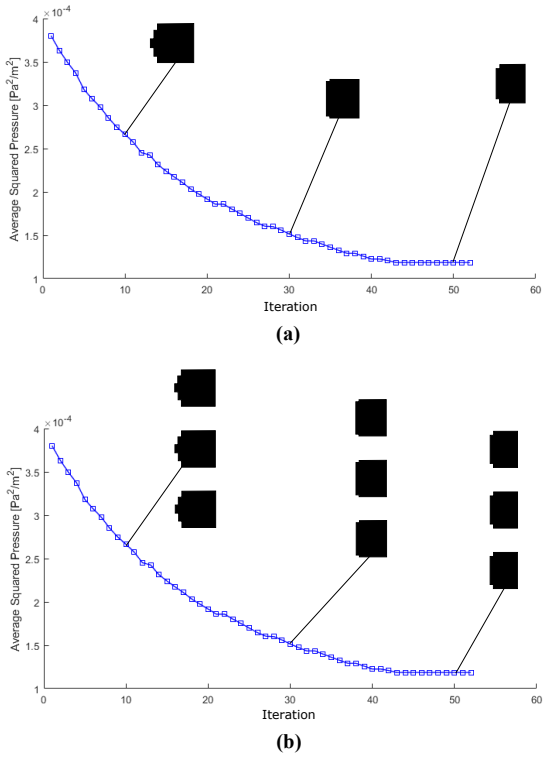

Figure 4. Objective function and barrier evolutions **(a)** one periodic cell **(b)** three periodic cells

From Fig. 5(b) it is noticed that the barrier converged to a non-symmetrical optimized form, completely different from the one presented in Fig. 3(c), even though its periodicity is maintained by the optimization method. This observation implies that, for the case of non-periodic boundaries, the optimization needs to be made for the whole fluid domain and not only for a small portion of it, as previously discussed. Additionally, the barrier may present some irregular behavior throughout the iterative procedure, due to abrupt variations of the objective function when the swap air-rigid is made. Sometimes, even elements located inside the barrier are turned to air, which does not affect the objective function at first, but sudden variations are usually observed when these elements meet the design domain surface. In this sense, the BESO parameters needed to be changed in order to slow down the optimization process and, therefore, reduce pressure variations.

Fig. 6 shows the evolution of the objective function with a presentation of the topologies for the 9th, 45th, 81st and 117th iterations. When looking at Fig. 4 and 6 it is noted that the number of iterations of the second case more than doubled in comparison to the first, showing an increase in computational cost. Despite that, the BESO method presents a reduction of the average square pressure by 83.39%, while the barrier suffers a 35% volume reduction.

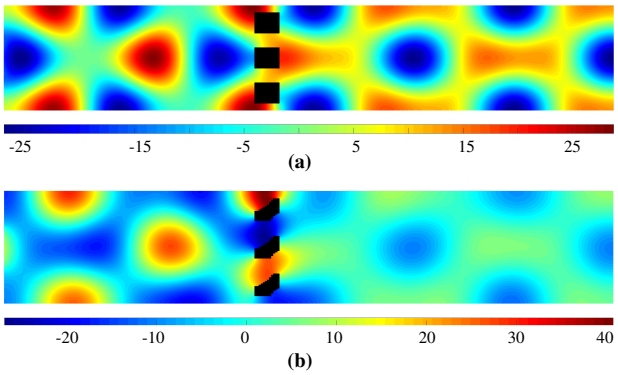

Figure 5. **(a)** Sound pressure field of an acoustic tube with a 45 mm cylindrical input **(b)** optimized result

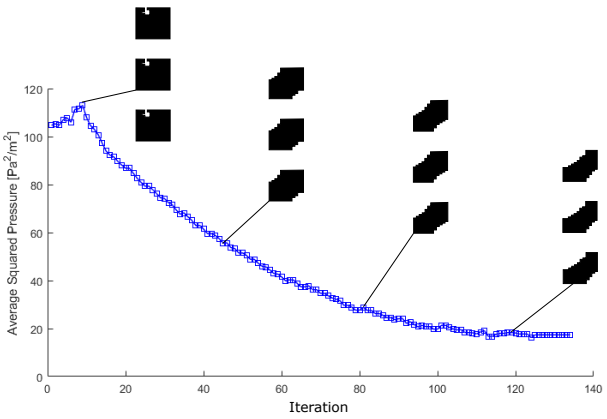

Figure 6. Evolution of the objective function for the non-symmetric case

goal of finding the best distribution of air ($\chi = 0$) and rigid ($\chi = 1$) elements in the design domain, thus building the most suitable noise barrier for the applications considered. The first case used one and three periodic cells. It is shown that the optimized results are, as expected, independent from the number of cells used, since the entire domain remained periodic, representing a low computational cost scenario. Additionally, the objective function has been reduced by 68.80%, with smooth behavior during the optimization procedure. In the second case, non-periodic inputs were examined. This made clear that, in those types of scenarios, the optimization needs to be made considering the entire acoustic tube, or Floquet-Bloch boundary conditions would have to be applied. In addition, BESO parameters were also required to change in order to deal with the abrupt variations of the evolutionary procedure. Despite of that, the objective function was reduced by 83.39% while the barrier volume decreased by 35%, showing that BESO is an applicable method to be used for the optimization of rigid acoustic barriers subjected to periodic and non-periodic conditions.

5. CONCLUSIONS

In this paper the Bi-directional evolutionary structural optimization (BESO) methodology was implemented with the

6. ACKNOWLEDGMENTS

The authors would like to thanks the financial support given by FAPESP (Fundação de Amparo à Pesquisa do

Estado de São Paulo), project number 2013/08293-7, and CAPES (Coordenação de Aperfeiçoamento de Pessoal do Nível Superior), finance code 001.

7. REFERENCES

[1] Y. M. Xie and G. P. Steven, "A simple evolutionary procedure for structural optimization," *Computers & structures*, vol. 49, no. 5, pp. 885–896, 1993.

[2] L. Xia, Q. Xia, X. Huang, and Y. M. Xie, "Bi-directional evolutionary structural optimization on advanced structures and materials: a comprehensive review," *Archives of Computational Methods in Engineering*, vol. 25, no. 2, pp. 437–478, 2018.

[3] X. Yang, Y. Xie, G. Steven, and O. Querin, "Bidirectional evolutionary method for stiffness optimization," *AIAA journal*, vol. 37, no. 11, pp. 1483–1488, 1999.

[4] X. Huang and M. Xie, *Evolutionary Topology Optimization of Continuum Structures: methods and applications*. West Sussex, UK: John Wiley & Sons, 1 ed., 2010.

[5] X. Huang and Y. Xie, "Convergent and mesh-independent solutions for the bi-directional evolutionary structural optimization method," *Finite Elements in Analysis and Design*, vol. 43, no. 14, pp. 1039–1049, 2007.

[6] X. Huang and Y.-M. Xie, "A further review of eso type methods for topology optimization," *Structural and Multidisciplinary Optimization*, vol. 41, no. 5, pp. 671–683, 2010.

[7] J. Kook, K. Koo, J. Hyun, J. S. Jensen, and S. Wang, "Acoustical topology optimization for zwicker's loudness model–application to noise barriers," *Computer Methods in Applied Mechanics and Engineering*, vol. 237, pp. 130–151, 2012.

[8] M. B. Dühring, J. S. Jensen, and O. Sigmund, "Acoustic design by topology optimization," *Journal of sound and vibration*, vol. 317, no. 3-5, pp. 557–575, 2008.

[9] J. W. Lee and Y. Y. Kim, "Rigid body modeling issue in acoustical topology optimization," *Computer methods in applied mechanics and engineering*, vol. 198, no. 9-12, pp. 1017–1030, 2009.

[10] J. W. Lee and Y. Y. Kim, "Topology optimization of muffler internal partitions for improving acoustical attenuation performance," *International journal for numerical methods in engineering*, vol. 80, no. 4, pp. 455–477, 2009.

[11] W. Vicente, R. Picelli, R. Pavanello, and Y. Xie, "Topology optimization of frequency responses of fluid–structure interaction systems," *Finite Elements in Analysis and Design*, vol. 98, pp. 1 – 13, 2015.

[12] R. Picelli, W. M. Vicente, R. Pavanello, and Y. Xie, "Evolutionary topology optimization for natural frequency maximization problems considering acoustic–structure interaction," *Finite Elements in Analysis and Design*, vol. 106, pp. 56–64, 2015.

[13] J. Kook, "Evolutionary topology optimization for acoustic-structure interaction problems using a mixed u/p formulation," *Mechanics Based Design of Structures and Machines*, vol. 47, no. 3, pp. 356–374, 2019.

[14] C. B. Dilgen, S. B. Dilgen, N. Aage, and J. S. Jensen, "Topology optimization of acoustic mechanical interaction problems: a comparative review," vol. 60, pp. 779–801, 2019.

[15] F. M. Azevedo, M. S. Moura, W. M. Vicente, R. Picelli, and R. Pavanello, "Topology optimization of reactive acoustic mufflers using a bi-directional evolutionary optimization method," *Structural and Multidisciplinary Optimization*, vol. 58, no. 5, pp. 2239–2252, 2018.

[16] N. Atalla and F. Sgard, *Finite Element and Boundary Methods in Structural Acoustics and Vibration*. Boca Raton, FL: CRC Press, 2015.

[17] R. D. Cook, D. S. Malkus, M. E. Plesha, and R. J. Witt, *Concepts and Applications of Finite Element Analysis*. John wiley & sons, 2002.

[18] W. U. Yoon, J. H. Park, J. S. Lee, and Y. Y. Kim, "Topology optimization design for total sound absorption in porous media," *Computer Methods in Applied Mechanics and Engineering*, vol. 360, p. 112723, 2020.

[19] D. A. Tortorelli and P. Michaleris, "Design sensitivity analysis: overview and review," *Inverse problems in Engineering*, vol. 1, no. 1, pp. 71–105, 1994.

[20] C. S. Jog and R. B. Haber, "Stability of finite element models for distributed-parameter optimization and topology design," *Computer methods in applied mechanics and engineering*, vol. 130, no. 3-4, pp. 203–226, 1996.

[21] K. Miyata, Y. Noguchi, T. Yamada, K. Izui, and S. Nishiwaki, "Optimum design of a multi-functional acoustic metasurface using topology optimization based on zwicker's loudness model," *Computer Methods in Applied Mechanics and Engineering*, vol. 331, pp. 116–137, 2018.

[22] F. I. Silva and R. Pavanello, "Synthesis of porous–acoustic absorbing systems by an evolutionary optimization method," vol. 42, pp. 887–905, 2010.

[23] J. S. Lee, P. Göransson, and Y. Y. Kim, "Topology optimization for three-phase materials distribution in a dissipative expansion chamber by unified multiphase modeling approach," vol. 287, pp. 191–211, 2015.